

# Simulation of Integrated Transmission and Distribution Networks with a Hybrid Three-Phase/Single-Phase Formulation

Glauco N. Taranto

José Mauro T. Marinho

FEDERAL UNIVERSITY OF RIO DE JANEIRO – COPPE  
RIO DE JANEIRO, BRAZIL

**Abstract**— This paper presents a simulation tool for transient stability analysis for integrated transmission and distribution networks, using hybrid positive-sequence and three-phase formulations. Extra High Voltage (EHV) transmission networks are assumed balanced and represented with positive-sequence models. Meshed high voltage (HV) and radial medium (MV) and low voltage (LV) distribution networks are represented with three-phase models in phase components. The paper builds upon the author’s work [1] related to a hybrid three-phase single-phase power flow formulation. Generic dynamic three-phase photovoltaic generation models are also proposed.

**Keywords** — Three-Phase Power Flow, Unbalanced Systems, Transient Stability, Hybrid single/three phase formulation, Three-Phase Photovoltaic Models.

## I. INTRODUCTION

The interest in the subject of electric energy generation by wind and solar renewable sources has been large in the last few years or decade. This non-dispatchable generation, which is largely connected not only to radial MV and LV distribution networks, but also to meshed HV distribution networks (known as subtransmission in North America), brings into the discussions the need for greater collaboration between the transmission system operator (TSO) and the distribution system operator (DSO). This fact is already observed in countries whose use of this type of generation is at a more advanced stage in comparison to other countries [2]. Looking at what is going on in those countries may avoid failures for the countries behind schedule.

A stronger integration of TSO and DSO in terms of electrical, economical and informational issues motivates the update, or even appearance, of computational tools capable of adequately analyze the behavior of both networks together. This trend of combining the transmission and distribution networks in new computational tools has gained greater attention lately, as it can be observed in the large number of publications [3-8] tackling the problem.

This paper presents a hybrid transient stability simulation tool where one part of the network (the transmission) is represented by positive-sequence models and the other part (the distribution) is represented by three-phase models. The

transient stability tool is built upon the hybrid three-phase/single-phase power flow solver proposed in [1].

The paper also shows an extension of the generic solar photovoltaic (PV) models, proposed in [11], to a three-phase representation.

## II. HYBRID POWER FLOW FORMULATION

In [1] we proposed a hybrid three-phase/single-phase power flow formulation, namely, in this paper, as *MonoTri* formulation. The single-phase representation is actually the conventional positive-sequence formulation used in traditional load flow solvers. The three-phase representation is formulated in phase components, instead of the most commonly used sequence components. However, to better summarize the basic ideas of the *MonoTri* formulation proposed in [1], we refer the reader to Fig.1 where the interface buses  $k$  and  $m$  are represented in sequence components. Between buses  $k$  and  $m$  there is the interface branch, which is either a transmission line or a transformer, represented by their  $\pi$ -equivalent model in sequence components.

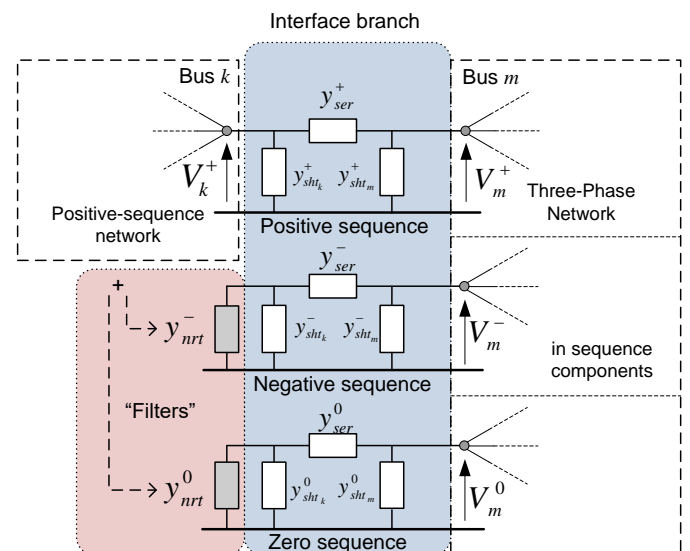


Fig. 1. Sequence components *MonoTri* interface

In Fig.1 Bus  $m$  and the interface branch are within the three-phase network, whereas Bus  $k$  is in the positive-sequence

The authors would like to express their gratitude to CNPq, CAPES and FAPERJ for their financial support.

network. Assuming that the three-phase network is balanced, there is no need to include the negative- and zero-sequence “filters”  $y_{nrt}^-$  and  $y_{nrt}^0$ , respectively, since there is no negative and zero sequence current components flowing into the positive-sequence network. However, if there are unbalances in the three-phase network, the negative and zero sequence “filters”  $y_{nrt}^-$  and  $y_{nrt}^0$  must be included in the interface branch as shown in Fig.1. This formulation allows the transmission (positive sequence) and the distribution (three-phase) networks to be solved simultaneously using the classic full Newton-Raphson method with quadratic convergence rate, as demonstrated in [1].

The concepts shown in Fig.1 can be extended to three-phase networks represented in phase components as shown in Fig.2. According to Fig.2, in the *MonoTri* formulation Bus  $k$  is represented only with the positive sequence component and Bus  $m$  is represented in  $a$ - $b$ - $c$  phase components.

A comprehensive formulation of the *MonoTri* interface elements in phase components is described in [1].

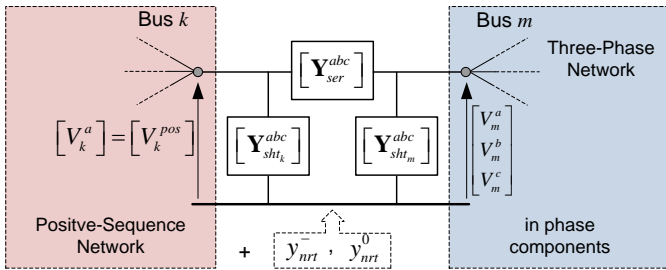


Fig. 2. Phase components *MonoTri* interface

Fig.3 shows how the hybrid *MonoTri* system would appear if the meshed EHV and HV networks would be kept represented in positive-sequence components, and the radial MV feeders would be represented in three-phase components. All generating units are represented by Norton equivalents.

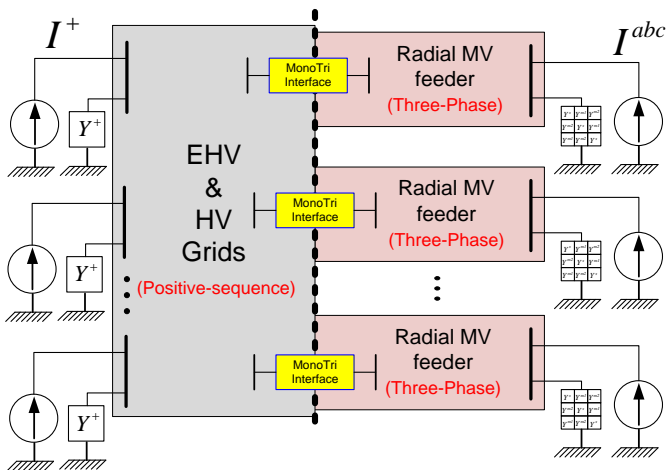


Fig. 3. *MonoTri* system with meshed network in positive-sequence component and radial feeders in three-phase component

Fig.4 shows how the hybrid *MonoTri* system would appear if only the EHV would be kept represented in positive-sequence components. In this case the three-phase network would also have a meshed part (HV) together with the radial MV and LV feeders. For this case, the *MonoTri* interface would have

transfer admittances connecting the interface buses as shown in Fig.5.

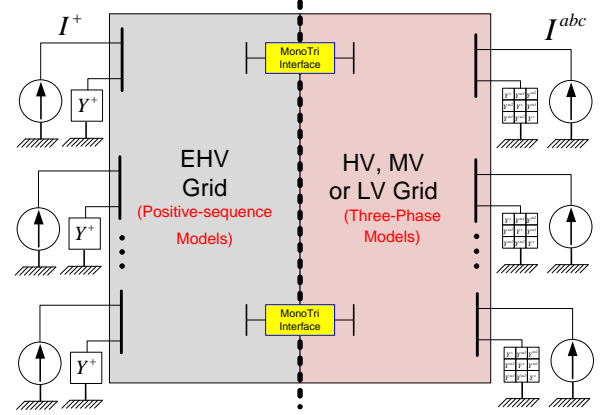


Fig. 4. System with meshed networks at both sides of the *MonoTri* interface

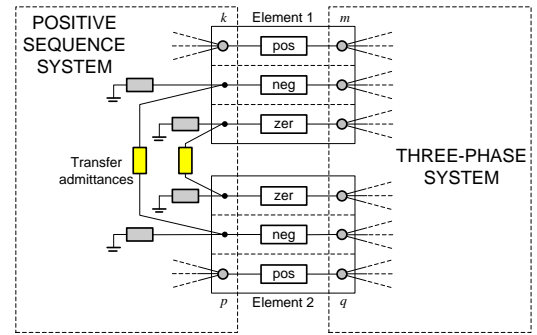


Fig. 5. Transfer negative and zero sequence admittances for meshed networks at both sides of the *MonoTri* interface

#### A. Static Three-Phase Modeling

Due to space limitation, this paper shows only the Norton representation of a three-phase voltage-controlled bus in the three-phase load flow solver, as seen in Fig.6. The function  $f_v(V^a, V^b, V^c)$  represents a sensor that measures the voltages of phases  $a$ ,  $b$  and  $c$ , at the terminal bus and outputs any combination of the phase voltages ( $V_{reg}$ ), e.g., the positive sequence voltage, the phase-to-phase voltages, etc.

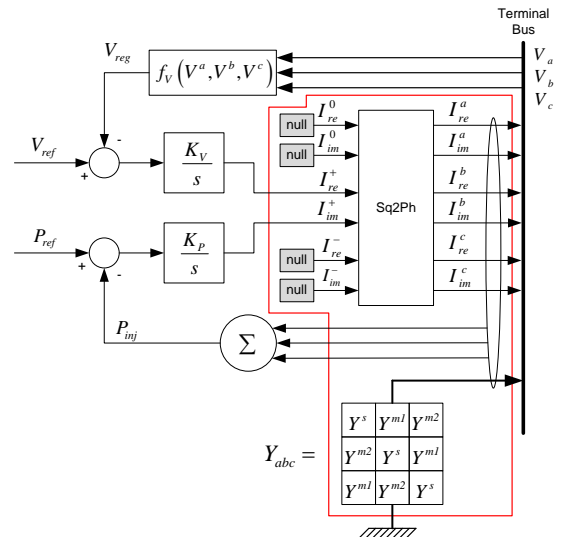


Fig. 6. Three-phase model of the voltage-controlled bus for load flow analysis

$V_{reg}$  is compared to a reference voltage ( $V_{ref}$ ) and the error is “integrated” by  $K_V/s$  thus giving rise to the real part of the positive-sequence current. A similar mechanism is made for the regulated active power injected at the generator bus ( $P_{inj}$ ).  $P_{inj}$  is calculated by using the injected currents in phase components, the phase voltages at the terminal bus, and the active power through the Norton admittance matrix. Thus,  $P_{inj}$  is compared to a reference power ( $P_{ref}$ ) and the error is “integrated” by  $K_P/s$  giving rise to the imaginary part of the positive-sequence current. Fig.6 also shows that the negative and zero sequence components of the generator is null, since generating units are built to create only balanced quantities. The values of  $K_V$  and  $K_P$  are not relevant in steady-state condition. The Norton admittance matrix in sequence components is given by (1).

$$Y^{0+-} = \begin{bmatrix} Y^0 & 0 & 0 \\ 0 & Y^+ & 0 \\ 0 & 0 & Y^- \end{bmatrix} \quad (1)$$

According to [9], and followed by this work, the positive-sequence impedance can be an arbitrary value, since there is a positive-sequence voltage behind it. To help convergence a small value should be chosen. The actual template values for the negative- and zero-sequence impedances are used. Additionally, if the saturated subtransient reactance is utilized, the model becomes readily adequate to short-circuit analysis. However, this subject is out of the focus of this paper, thus being a subject of a future publication.

Once defined the sequence-component admittances, matrix (1) is transformed to phase components according to (2).

$$Y^{abc} = T \times Y^{0+-} \times T^{-1} \quad (2)$$

where,

$$T = \begin{bmatrix} 1 & 1 & 1 \\ 1 & a^2 & a \\ 1 & a & a^2 \end{bmatrix} \quad (3)$$

is the sequence to phase matrix transformation, represented by the block Sq2Ph shown in Fig.6, and  $a$  is the complex operator  $e^{j2\pi/3}$ . Therefore, the three-phase Norton admittance matrix in phase components is given by (4).

$$Y^{abc} = \begin{bmatrix} Y^s & Y^{m_1} & Y^{m_2} \\ Y^{m_2} & Y^s & Y^{m_1} \\ Y^{m_1} & Y^{m_2} & Y^s \end{bmatrix} \quad (4)$$

Similar representations are made for the  $V\theta$  and  $PQ$  buses, where the corresponding regulated quantities are “integrated” and positive-sequence current injections are found.

### III. HYBRID TRANSIENT STABILITY FORMULATION

The mathematical formulation of the three-phase transient stability (TS) solver is the same as of the conventional positive-sequence TS solver. However, special attention must

be given to the three-phase dynamic models of generators, induction machines, FACTS devices, and their interfaces with the three-phase network represented in phase components.

The conventional differential-algebraic equations (5) are utilized:

$$\begin{aligned} \dot{x} &= f(x, V) \\ 0 &= g(x, V) \end{aligned} \quad (5)$$

where  $x$  represents the vector of state variables,  $V$  the vector algebraic variables,  $f$  the set of nonlinear differential equations and  $g$  the set of nonlinear algebraic equations.

Again due to space limitation, this paper shows only the dynamic representation of a three-phase synchronous machine, which is connected to a voltage-controlled bus for the TS solver, as seen in Fig.7. It is possible to note similarities in the voltage-controlled bus models depicted in Figs. 6 and 7.

A comprehensive analysis of the synchronous machine behavior operating in unbalanced conditions at fundamental frequency is given in [10].

The Park model uses only the  $dq$ -components of the positive sequence voltage transformed by the blocks Ph2sq and ri2dq shown in Fig.7. The model considers an extra torque (represented by  $T$ ) in the rotor swing equation for the unbalanced case, approximately capturing the braking effects of the negative sequence armature current. Armature zero sequence current will only flow if the machine is Y-grounded connected. Even though synchronous machines normally are grounded by impedances, they are also normally connected to the grid by a step-up  $\Delta$ -Y transformer, which isolates the machine to the zero sequence. Therefore, we neglect the dynamics due to zero sequence components in the machine model. The armature currents in  $dq$ -components are the outputs of the Park Model (see Fig.7). They are firstly transformed to positive-sequence current injections by the dq2ri block, and secondly transformed to phase component current injections at the machine terminal bus. Likewise the static model shown in Fig.6, the negative and zero-sequence current injections are also null in the dynamic model.

The only connection of the dynamic model of the machine and the unbalanced conditions of the grid resides in the rotor swing equation. The negative-sequence torque is given by (6).

$$T^- = (R^- - R^+) (I^-)^2 = G^- (V^-)^2 \left( 1 - \frac{R^+}{R^-} \right) \quad (6)$$

where  $R^+$  is the positive sequence armature resistance and  $R^-$ ,  $I^-$  and  $G^-$  and  $V^-$  are the negative sequence resistance, current, conductance and voltage, respectively. The net torque in the swing equation thus becomes:

$$T_{net} = T_{mec} - T^+ - T^- - D\omega \quad (7)$$

Therefore, any detailed cylinder or salient-pole machine models, exciter, voltage regulator, turbine and speed regulator models can be accommodated with the approximations confined in the rotor swing equation. This is computationally very attractive since with minor modifications all legacy dynamic model libraries can be readily utilized in our proposed hybrid TS solver.

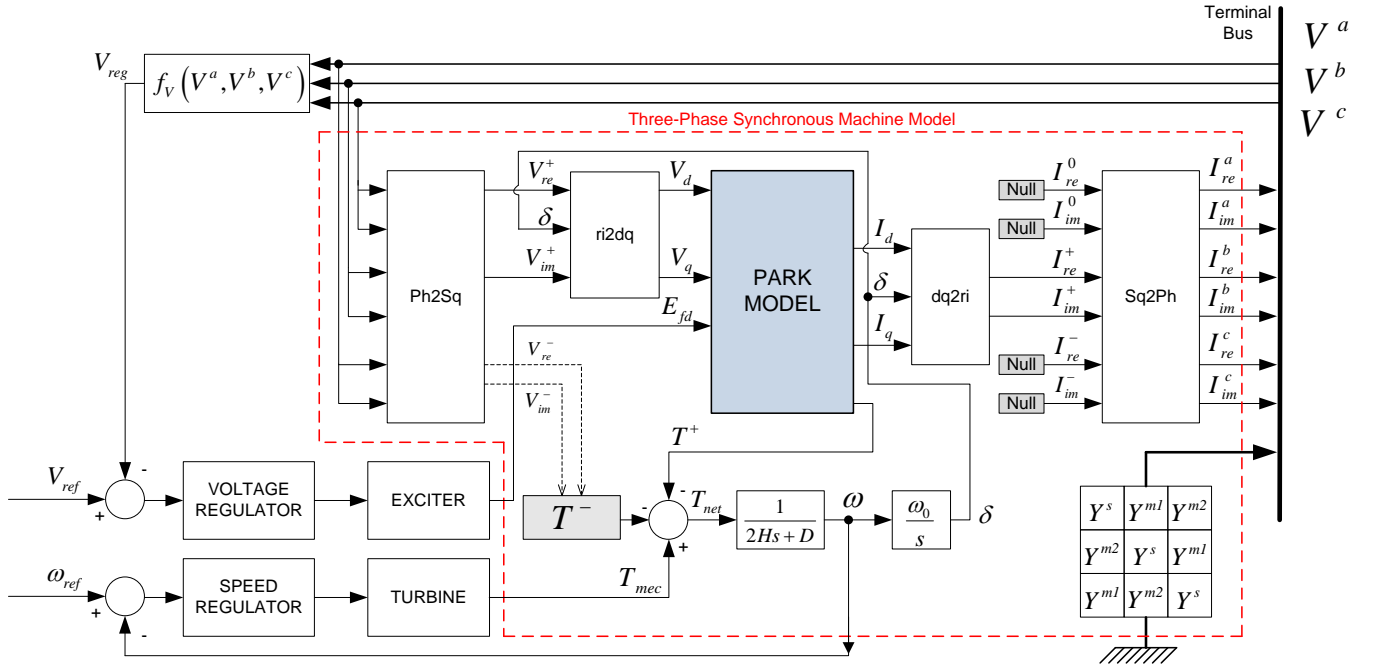


Fig. 7. Three-phase model of the synchronous machine for transient stability analysis

#### IV. THREE-PHASE GENERIC PHOTOVOLTAIC (PV) MODELS

One of our biggest motivations to come up with the *MonoTri* formulation for load flow and transient stability analysis was the widespread usage of distributed renewable generation connected to distribution networks (HV, MV and LV) via electronic inverters. Therefore, wind and PV solar generators are of particular interest. The *MonoTri* formulation was the strategy to continue using the positive-sequence static and dynamic models database commonly found in TSO's computational systems, together with the three-phase database adopted in DSO's computational systems.

Reference [11] proposed generic positive-sequence fundamental frequency PV generation models to be utilized in electromechanical TS programs. This paper extends those models to three-phase representation, according to the structure presented in Fig.8, combined with the models shown in the appendix.

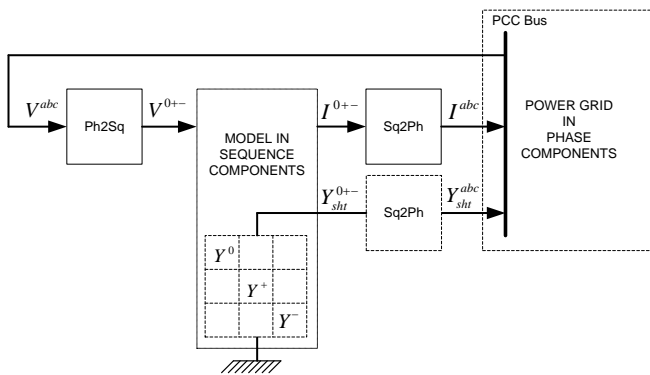


Fig. 8. Three-phase current-source in sequence components

The major modification with respect to the positive-sequence models is on the injected currents at the point of common

coupling (PCC) bus. The three-phase model remains a controlled current source represented as a Norton equivalent.

Recognizing that the majority of existing three-phase PV inverters is three-legged and connected to the grid by a transformer with a  $\Delta$  winding in either side,  $Y^0$  is equal to zero. The positive-sequence impedance of the PV generator is mainly the output inductive filter that is not represented in our model. Therefore,  $Y^+$  assumes a very large number. The inverter can be programmed to give the negative admittance  $Y^-$  any value between zero and infinity [12,13]. Therefore, to model an ideal three-phase current source, the triplet  $(Y^0, Y^+, Y^-)$  should be  $(0, \infty, 0)$ . Once the admittance triplet is defined, the admittance matrix in phase components is given by (4).

#### Asymmetrical current injection

Contrary to synchronous machines where negative sequence impedance is inherently low, inverter-based DG is typically programmed to produce positive-sequence quantities, thus becoming an open-circuit for the negative sequence current. However, the ideal triplet  $(Y^0 = 0, Y^+ = \infty, Y^- = 0)$  can be altered as inverters can be programmed to inject asymmetrical currents, thus creating a finite impedance path to the negative sequence current [12].

Fig.9 shows the generic three-phase PV generator resembling the positive-sequence generic model given in [11]. The function  $f_V(V^a, V^b, V^c)$ , similar to the one described in Fig.6, measures the phase voltages at the PCC bus.

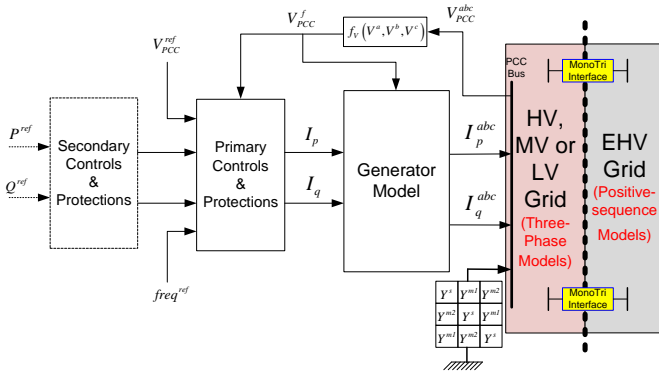


Fig. 9. Three-phase generic PV model

The three-phase PV model has exactly the same protection and control functions described in [11], and reproduced in Fig.15 for the PVD1 model in the appendix. The Primary Controls & Protections block is utilized in concentrated and distributed PV plants. The Secondary Controls & Protections block is utilized only in concentrated PV plants to represent a supervisory layer.

## V. SIMULATING RESULTS

The hybrid *MonoTri* formulation was tested in a 730-bus equivalent of the Brazilian Interconnected Power System (BIPS) as depicted in Fig.10. The system has 116 generating (voltage-controlled) buses, from which 82 generating units are dynamically represented for TS analysis.

For comparison purposes, we have considered three different representations for the transient stability analysis:

- i) All 730 buses represented as single phase (positive sequence);
- ii) All 730 buses represented as three phases;
- iii) *MonoTri* formulation with only 58 buses represented with three phases, and the rest as single phase.

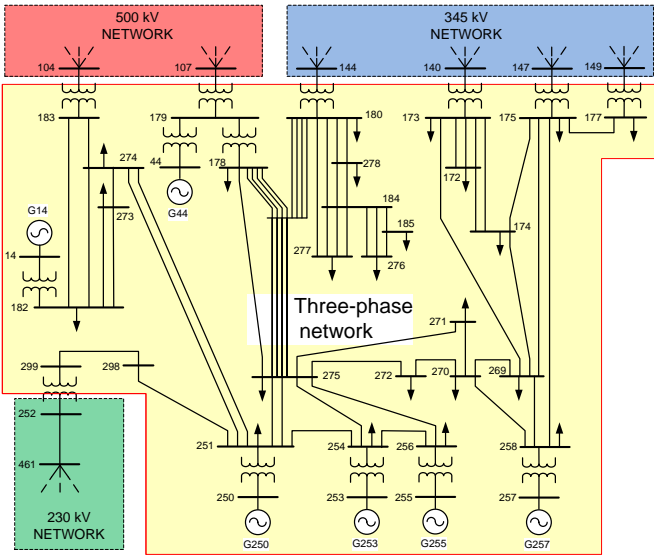


Fig. 10. Part of the BIPS under *MonoTri* formulation

Fig.10 shows 35 out of the 58 three-phase-represented buses for Case iii in the yellow part. The 58 buses were chosen

according to their voltage levels, being less or equal to 138 kV. Lower voltage buses are not drawn in Fig.10. The 58 buses comprise the HV and some equivalent MV feeders of a distribution utility in the BIPS.

The dynamic components within the three-phase-represented network in Case iii are five synchronous generators, one synchronous condenser and their voltage and speed regulators. The *MonoTri* interfaces are also shown in Fig.10 in 7 locations, two 500 kV buses (Buses 104 and 107), four 345 kV buses (Buses 140, 144, 147 and 149) and one 230 kV bus (Bus 461). In 6 locations the interface branches are transformers and in 1 location it is a transmission line (461-252). For this example there are no solar PV plants in the system.

### A. Balanced System Analysis

Ideally the simulations for Cases i, ii and iii are identically the same when the system is balanced. In order to benchmark the results, a commercial grade positive-sequence transient stability program heavily utilized in Brazil was also used for comparison purposes.

The simulation consisted of a three-phase fault applied in Bus 272 for 100 ms. Fig.11 shows the machine rotor angle of generating unit G253.

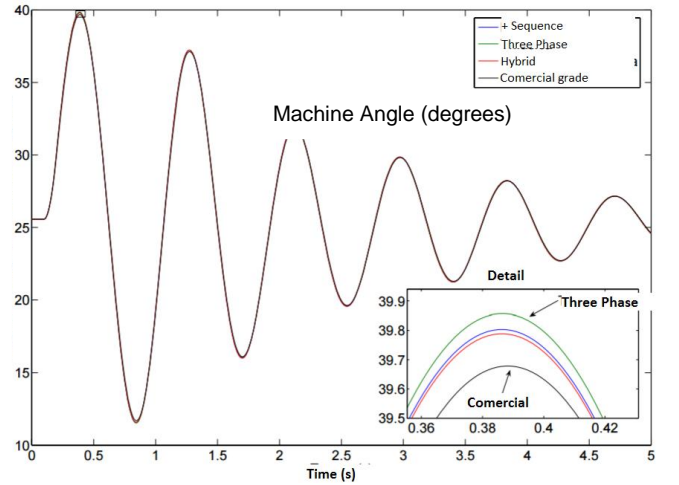


Fig. 11. Machine angles in four simulations: Case i (blue); Case ii (green), Case iii *MonoTri* formulation (red) and Commercial grade software (black).

Only in the zoomed window highlighting the peak of the first swing, one can note the small differences among the four simulations. The largest difference encountered was 0.2 degree. This difference is due to tolerances in integration methods and numerical truncation errors.

### B. Unbalanced System Analysis

#### Load Flow Analysis

For the unbalanced system we have performed analyses only to the full three-phase representation (Case ii) and the *MonoTri* representation (Case iii). For Case iii, no negative and zero sequence “filters”  $y_{nrt}^-$  and  $y_{nrt}^0$  were considered, meaning that the Newton-Raphson solver will converge to a solution where the there-phase quantities will have some degree of approximation.



The unbalance was created by connecting a  $\Delta$ -Yg (Delta - Y grounded) 100 MVA transformer at Bus 271 with 8% series reactance and a tap fixed at 0.96 pu, to mimic an HV/MV primary substation transformer. The original load (a balanced  $60+j14$  MVA) at Bus 271 was replaced to the secondary bus, namely, Bus S-271, with the connection Yg. Finally, the load connected to phase  $b$  was equally divided between phases  $a$  and  $c$ , leaving phase  $b$  with no load. The other loads in the system remained  $\Delta$ -connected balanced at the 138 kV buses. This avoided the representation of the HV/MV transformers and filtered out zero sequence unbalances into the 138 kV network, resembling a real life situation.

Table I shows the load flow solution for the voltage at the HV Bus 271 and at the MV Bus S-271. The obtained results show errors less than 0.33% in the voltage magnitude ( $E_V$ ) and less than  $0.2^\circ$  in the phase angle ( $E_\theta$ ).

Table I – Errors at Buses 271 and S-271

Bus		Full Three Phase			MonoTri			Error	
#	Phase/Seq.	pu	°	MVA	pu	°	MVA	$E_V$ (%)	$E_\theta$ (°)
271	$a$	0.955	0.4		0.956	0.5		0.10	0.2
	$b$	0.953	-118.7		0.955	-118.7		0.20	-0.1
	$c$	0.968	120.9		0.965	120.9		-0.31	0.0
S-271	$a$	0.974	26.6	$30+j7$	0.978	26.6	$30+j7$	0.33	0.1
	$b$	1.008	-88.6	$30+j7$	1.007	-88.8	$30+j7$	-0.11	-0.2
	$c$	0.990	146.3	$30+j7$	0.988	146.4	$30+j7$	-0.21	0.1

### Transient Stability Analysis

The system was pre-fault balanced. Unbalance is only due to an unbalanced fault. The simulation consisted of a two-phase fault (phases  $b$  and  $c$ ) applied in Bus 258 for 150 ms. Since the three-phase modeling is based on phase components, it is straightforward to represent any kind of unbalanced fault.

Fig.12 shows rotor angles, in degrees, of generators G14, G250, G255 and G257. The solid red plots represent the simulation for Case ii, where the whole system is represented with three-phase models, and the dashed blue plots represent the simulation for Case iii, where the *MonoTri* formulation is adopted. One can note that there is a very good match between the two cases, especially for those machines far away from the faulted bus. Since the negative and zero sequence filters are ideal, i.e., equal to infinity, the simulations done with the *MonoTri* formulation present some approximations.

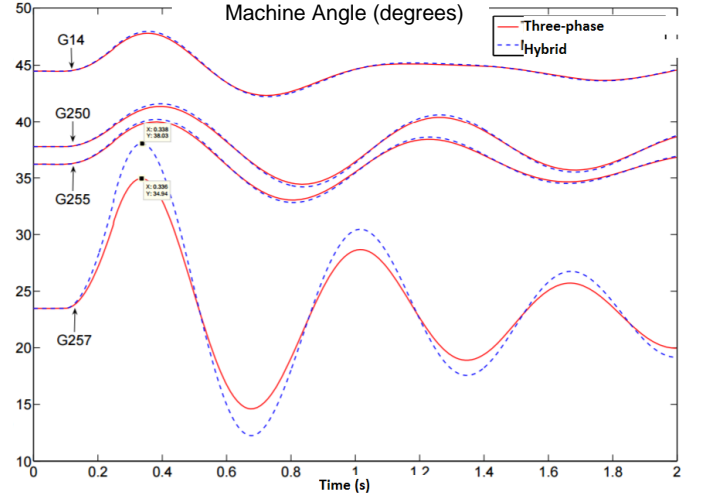


Fig. 12. Machine angles in two simulations: Case ii (solid red); Case iii (dashed blue).

Fig.13 shows the phase voltages, in pu, of Bus 258 for Case ii (solid red) and Case iii (dashed blue). One can note that there are some visual discrepancies only during the short-circuit period, since the pre-fault and post-fault networks are balanced. The largest error in the voltage is 3% in phase  $a$  during the fault.

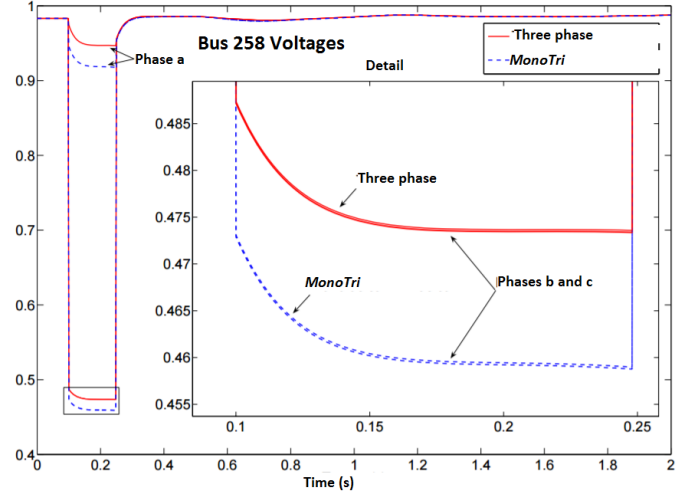


Fig. 13. Phase voltages of Bus 258 in two simulations: Case ii (solid red); Case iii (dashed blue).

## VI. CONCLUSIONS

This paper built upon a hybrid three-phase/single-phase power flow formulation proposed in [1], namely, in this paper *MonoTri* formulation. In this paper the *MonoTri* formulation was extended to a transient stability simulation tool. The paper presented results in a mid-size test system (730 buses) representing an equivalent of the Brazilian Interconnected Power System.

The paper also extended the representation of the generic models of inverter-based generation proposed in [11], to a three-phase formulation with the grid in phase components.

## REFERENCES

- [1] J. M. T. Marinho & G. N. Taranto, "A Hybrid Three-Phase Single-Phase Power Flow Formulation," *IEEE Transactions on Power Systems*, Vol. 23, No. 3, pp. 1063-1070, August 2008.
- [2] H. Doring, D. Engelbrecht, H. Bock, G. Scheibner & O. Ziemann, "Increased cooperation between TSO and DSO as precondition for further developments in ancillary services due to increased distributed (renewable) generation", *CIGRÉ Session*, Paper C2-111, Paris, 2016.
- [3] H. Sun, Q. Guo, B. Zhang, Y. Guo, Z. Li, and J. Wang, "Master-Slave-Splitting based distributed global power flow method for integrated transmission and distribution analysis," *IEEE Transactions on Smart Grid*, vol.6, no. 3, pp. 1484-1492, 2015.
- [4] H. P. Schmidt, J. C. Guaraldo, M. M. Lopes & J. A. Jardini, "Interchangeable Balanced and Unbalanced Network Models for Integrated Analysis of Transmission and Distribution Systems", *IEEE Transactions on Power Systems*, Vol. 30, No. 5, pp. 2747-2754, 2015.
- [5] P. Aristidou and T. Van Cutsem, "A parallel processing approach to dynamic simulations of combined transmission and distribution systems," *International Journal of Electrical Power & Energy Systems*, 72, pp.58-65. 2015.
- [6] B. Palmintier, E. Hale, B. M. Hodge, K. Baker & T. M. Hansen, "Experiences integrating transmission and distribution simulations for DERs with the Integrated Grid Modeling System (IGMS)", *Power System Computation Conference (PSCC)*, Genoa, Italy, 2016.
- [7] Q. Huang & V. Vittal, "Integrated Transmission and Distribution System Power Flow and Dynamic Simulation Using Mixed Three-Phase-Sequence/Three-Phase Modeling", *IEEE Transactions on Power Systems*, IEEE Xplore early access, 2017.
- [8] IEEE PES, "Contribution to Bulk System Control and Stability by Distributed Energy Resources Connected at Distribution Network", *Technical Report PES-TR22*, January 2017
- [9] J. Arrillaga & N. R. Watson, *Computer Modelling of Electrical Power Systems*, 2nd Edition, John Wiley & Sons, 2001.
- [10] P. Kundur, *Power System Stability and Control*, Chapter 13, McGraw-Hill, 1994.
- [11] WECC Renewable Energy Modeling Task Force, "WECC PV Power Plant Dynamic Modeling Guide", USA, April 2014.
- [12] E. Quitmann, M. Fischer, A. El-Deib & S. Engelken, "Anticipating Power System Needs in Response to the Global Energy Transition", *CIGRÉ Session*, Paper C2-114, Paris, 2016.
- [13] IEEE PES, "System Neutral Grounding Considerations for Inverter-Interfaced Distributed Energy Resources", *Technical Report PES-TR21*, December 2016.

## APPENDIX

Fig.14 (taken from [11]) shows the overall block diagram of the generic PV model that accounts for the concentrated and distributed PV generation. Fig.15 (also taken from [11]) shows the PVD1 generic model proposed for distributed solar PV.

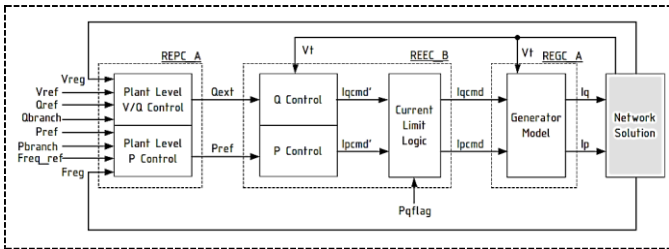


Fig. 14. Overall block diagram of the generic PV model proposed in [11].

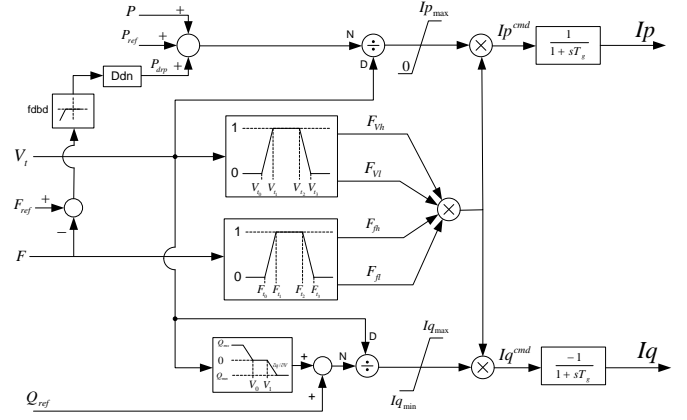


Fig. 15. PVD1 model proposed in [11].

The last block to the right in Fig.14, labeled *Network Solution*, represents the interface of the inverter to the power grid. It receives as inputs the currents proportional to the active and reactive powers decomposed in the  $p$  and  $q$  axes, respectively. Then it performs the angular reference transformation and solves the current injection equations at the inverter terminal bus. With a suitable modeling for the effects of the negative sequence on the inverter, this block can be extended to a three-phase representation of the electric network. For the zero sequence, however, no further consideration is required, since usually the inverters are three-wire open-Y connected, thus blocking zero sequence currents.